This is an accepted version of the paper. Please cite as: Abel, C. et al. The human–environment nexus and vegetation–rainfall sensitivity in tropical drylands. Nat Sustain 4, 25–32 (2021). https://doi.org/10.1038/s41893-020-00597-z

The human–environment nexus and vegetation–rainfall sensitivity in tropical drylands

Christin Abel[1], Stéphanie Horion[1], Torbern Tagesson[1,2], Wanda De Keersmaecker[3], Alistair W. R. Seddon[4,5], Abdulhakim M. Abdi[1,6] and Rasmus Fensholt[1]

Global climate change is projected to lead to an increase in both the areal extent and degree of aridity in the world's drylands. At the same time, the majority of drylands are located in developing countries where high population densities and rapid population growth place additional pressure on the ecosystem. Thus, drylands are particularly vulnerable to environmental changes and large-scale environmental degradation. However, little is known about the long-term functional response of vegetation to such changes induced by the interplay of complex human–environmental interactions. Here we use time series of satellite data to show how vegetation productivity in relation to water availability, which is a major aspect of vegetation functioning in tropical drylands, has changed over the past two decades. In total, one-third of tropical dryland ecosystems show significant ($P < 0.05$) changes in vegetation–rainfall sensitivity with pronounced differences between regions and continents. We identify population as the main driver of negative changes, especially for developing countries. This is contrasted by positive changes in vegetation–rainfall sensitivity in richer countries, probably resulting from favourable climatic conditions and/or caused by an intensification and expansion of human land management. Our results highlight geographic and economic differences in the relationship between vegetation–rainfall sensitivity and associated drivers in tropical drylands, marking an important step towards the identification, understanding and mitigation of potential negative effects from a changing world on ecosystems and human well-being.

Global drylands support approximately 30% of the world's population[1] and more than half of all birds and mammals[2], in addition to livestock and crops for global food production[3]. Understanding ecosystem dynamics in drylands is thus essential for the implementation of UN Sustainable Development Goal 15, life on land. As drylands are characterized by a limited availability of water[4], all living organisms have adapted to survive in these conditions. However, global climate change is leading to unprecedented alterations and shifts in the global climatology[5], causing extended droughts and regional warming[6,7] or resulting in changing rainfall patterns[8]. If the frequency and severity of climatic extremes continue to increase, ecosystem functioning, composition, biodiversity and soil properties[9–11] of many drylands will undergo adverse changes with increasingly limited capacity to be reversed[12]. In addition to climatic changes, drylands are facing an increase in anthropogenic pressure through, for example, deforestation or human land management (cropland expansion and intensification)[13–15]. Moreover, most dryland areas are located in developing countries, where people's livelihoods are directly dependent on the land and the ecosystem services this land provides, for example, food, fodder and timber supply (both for own use and export)[5]. Rapid population growth (especially affecting developing countries) and the associated increased need for food, agricultural area and infrastructure place additional pressure on the functioning of dryland ecosystems[16–18]. As drylands are projected to expand by up to 23% by the end of the twenty-first century[19], increasing aridity is expected to be more important in more-humid climatic zones[12,20], highlighting the importance of gaining a clearer understanding of dryland ecosystem functioning.

Ecosystem functioning is a broad term that describes how different ecosystem properties (for example, pools of organic matter or carbon) and processes (fluxes of energy and matter) interact to sustain the system over space and time[21,22], maintaining a state of dynamic equilibrium of disturbance and recovery[23]. As such, vegetation is a key aspect within the concept of ecosystem functioning as it absorbs carbon dioxide and provides a range of products people depend on. In drylands, where vegetation productivity is tightly linked to the availability of water, the sensitivity of vegetation to rainfall is one major factor of vegetation functioning. Thus, a quantification of the vegetation–rainfall relationship (VRR) has been established as a successful proxy for vegetation sensitivity to rainfall that can be used as a simplified indicator for vegetation functioning[1,24,25] and is applied here accordingly. Alterations in the VRR may indicate changes in vegetation biophysical processes in relation to water availability, potentially impacting ecosystem processes such as net primary productivity, carbon uptake and allocation and leading to changes in ecosystem functional traits[26].

Although a number of studies have used time series of remote-sensing-based vegetation and climatic data to analyse the vegetation response to climate anomalies in drylands[27–29], the patterns of changes over time at the global scale, and any associated changes in ecosystem and vegetation functioning, remain unknown. Similarly, several studies have already shown that the anthropogenic pressure on dryland ecosystems is growing and not negligible[30,31]. Yet, we have limited understanding of the ability of dryland vegetation to sustain functioning while coping with the combined impact of climate change and anthropogenic pressure. As such, we present a suite of analyses to better understand both the direction of

[1]Department of Geosciences and Natural Resource Management, University of Copenhagen, Copenhagen, Denmark. [2]Department of Physical Geography and Ecosystem Science, Lund University, Lund, Sweden. [3]Laboratory of Geo-Information Science and Remote Sensing, Wageningen University, Wageningen, the Netherlands. [4]Department of Biological Sciences, University of Bergen, Bergen, Norway. [5]Bjerknes Centre for Climate Research, Bergen, Norway. [6]Centre for Environmental and Climate Research, Lund University, Lund, Sweden. ✉e-mail: christin.abel@ign.ku.dk

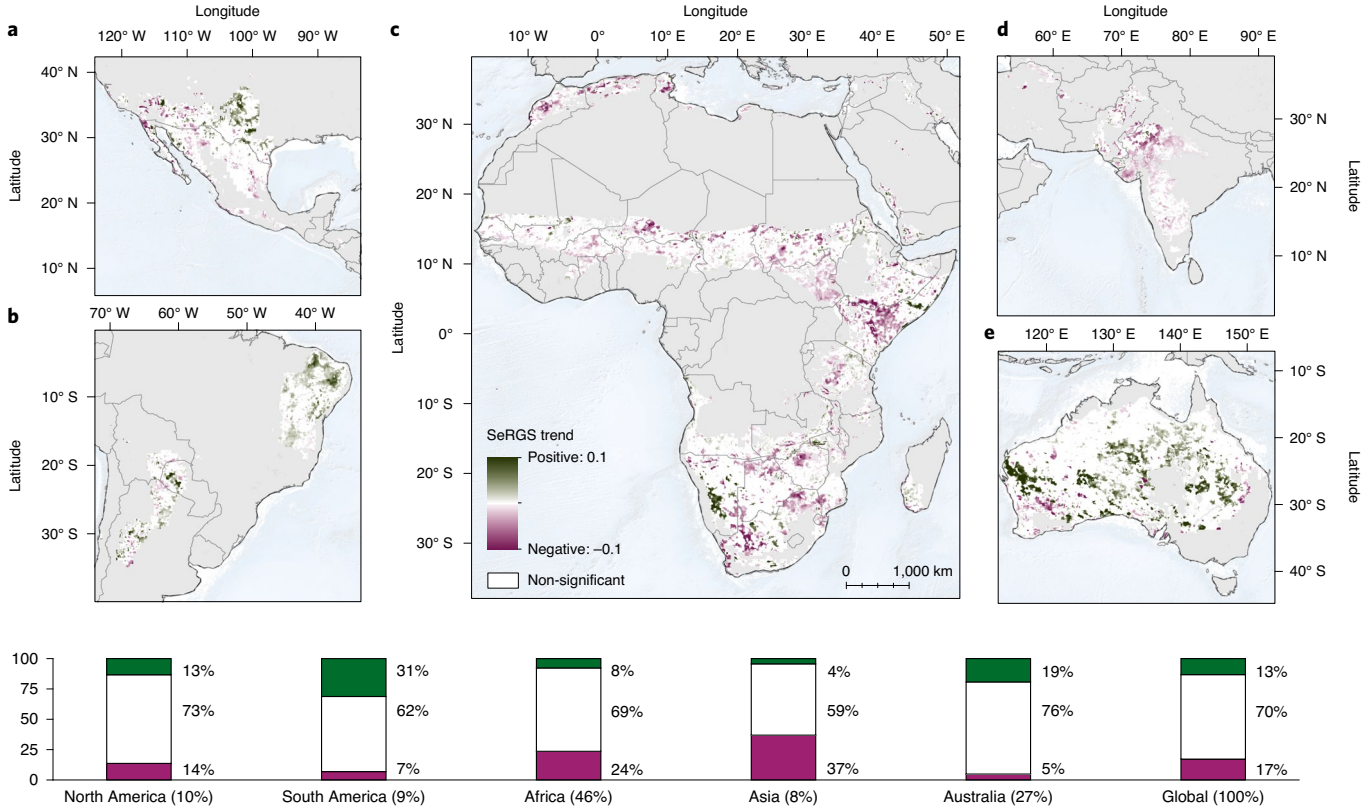

Fig. 1 | Significant positive and negative trends in vegetation–rainfall sensitivity (Mann–Kendall test, $P < 0.05$) across continents and their distribution per continent (and globally) in %. a, North America. **b**, South America. **c**, Africa. **d**, Asia. **e**, Australia. Numbers next to the continent names indicate their share of the tropical dryland area. Figure is based on all pixels within the dryland mask at 0.05° spatial resolution.

change with respect to the vegetation–rainfall sensitivity and the underlying drivers of change. As the VRR is strongest in tropical drylands and those regions account for 70–80% of all global arid and semi-arid areas[32], we are focusing on tropical drylands (see Methods) in this study.

Here, we use sequential linear regression slopes (SeRGS, see Methods)[25] as a proxy of vegetation sensitivity to rainfall in tropical drylands. We describe the VRR with a time series of remotely sensed metrics of vegetation productivity and rainfall. Through a successive spatio-temporal analysis of the VRR (using a moving window), the SeRGS approach is able to account for non-static changes in water availability and reveal potential changes in the VRR over time. Using this approach, we go beyond the traditional one-dimensional analyses of vegetation productivity changes and provide a more nuanced characterization of vegetation dynamics and functioning. We interpret positive/negative trends in SeRGS over time (that is, an increasing/decreasing VRR) as an increase/decrease in unit vegetation productivity (normalized for rainfall variability) per unit rainfall, indicative for changes in vegetation functioning. Building on previous satellite-based studies on vegetation responses[29] in dryland regions[27], we then relate the observed changes in vegetation–rainfall sensitivity to both climatic and anthropogenic stressors. We estimate the relative importance of these potential stressors and further assess their interconnectivity.

Continental differences in vegetation–rainfall sensitivity

We used metrics of vegetation productivity (Moderate Resolution Imaging Spectroradiometer (MODIS) Normalized Difference Vegetation Index (NDVI) and Vegetation Index and Phenology (VIP) data) and water availability (Multi-Source Weighted-Ensemble Precipitation (MSWEP) rainfall data) from 2000 to 2015 to calculate SeRGS over the tropical dryland area at 0.05° spatial resolution (Supplementary Fig. 1), indicative of changes in vegetation sensitivity to rainfall (see Methods). Our analysis revealed that approximately one-third (30%) of tropical drylands show significant trends (Mann–Kendall test, $P < 0.05$) in vegetation–rainfall sensitivity over the past two decades. This translates into 13% positive and 17% negative trends. In general, positive trends indicate that vegetation becomes more responsive to available rainfall over time. Negative trends point towards less-responsive vegetation and less vegetation productivity per available unit of rainfall, indicating a shift towards vegetation that may be impeded in its functioning. We observe pronounced continental differences in the distribution and direction of trends (Fig. 1) with Australia and South America showing the largest shares of positive trends, followed by substantially lower shares for Africa and Asia. Similarly, the largest fraction of negative trends is found across the tropical drylands of Asia (statistically different from all other continents), followed by Africa and parts of North America (Fig. 1).

To gain a better understanding of the observed trends and the potential drivers of the spatial/continental differences in the vegetation–rainfall sensitivity, we link the trends in SeRGS to a set of potentially related driver variables. While SeRGS in itself includes rainfall as the main driver of vegetation productivity (in tropical drylands) and accounts for rainfall interannual variations, other meteorological variables (MET) such as temperature and soil-water availability may influence vegetation biophysical processes (for example, favourable temperature conditions, less-frequent or severe climate extremes). Moreover, a range of other factors, such as population density (POP), vegetation cover (VC, based on vegetation cover fraction layers from ref. [33] (see Methods)) and fire occurrence (FIRE) are considered as potential driver variables. We use an empirical approach

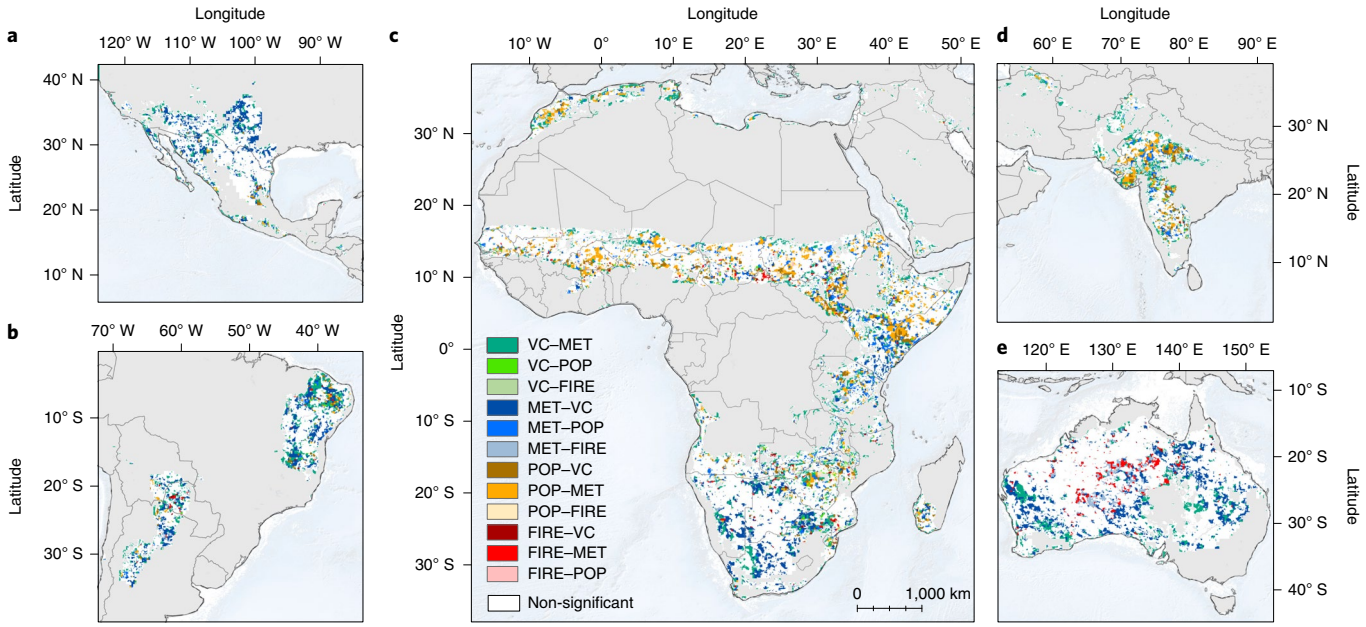

Fig. 2 | Main driver combinations of significant trends (Mann–Kendall test, $P < 0.05$) in vegetation–rainfall sensitivity per pixel at 0.25° spatial resolution. a, North America. **b**, South America. **c**, Africa. **d**, Asia. **e**, Australia. The first variable indicates the main driver and the second variable indicates the second (co-) driver. A map showing the main driver only is found in Supplementary Fig. 6.

based on principal component analysis (PCA) and regression (PCR) to model the contribution of the drivers to changes in vegetation sensitivity to rainfall (see Methods and Supplementary Fig. 5). The advantage of this approach is that any impact of collinearity between the driver variables has been removed, resulting in an independent estimate of the relative importance of each variable. At the global scale, we find that most of the significant trends in the vegetation–rainfall sensitivity are driven primarily by changes in climate (MET) (52.8%), followed by VC change (24.5 %), POP (18.7 %) and FIRE (4.03 %). Nowhere was any single driver variable found to be the unique determinant of the observed change in the vegetation–rainfall sensitivity, and clear continental differences in co-limitations were revealed through the analysis of the first and second driver variables on a per-pixel basis (Figs. 2 and 3).

Combinations in driver variables involving POP and MET are most frequent in Asia and Africa (Fig. 3b), and in both cases, they are related to negative changes in the vegetation–rainfall sensitivity (Fig. 3a). Climate, in combination with a change in vegetation cover, is predominantly driving positive changes (Fig. 3a) in North and South America as well as in Australia (Fig. 3b).

Climate as primary driver of vegetation–rainfall sensitivity

The most extensive regions driven primarily by climate (MET) emerge in North America, Australia and Southwest Africa, in which positive trends in vegetation–rainfall sensitivity are observed (Figs. 1–3 and Supplementary Fig. 6). We associate these positive trends with either an increase in vegetation cover or vegetation that is increasingly sensitive to rainfall. Similarly, other studies have reported a high sensitivity of vegetation to climatic variability, especially water availability[29] and low resilience (to short-term climatic anomalies)[28], in these regions on the basis of the analysis of monthly time series of vegetation and climate data. Since our model of vegetation–rainfall sensitivity (SeRGS) normalizes vegetation productivity for interannual variations in rainfall, the observed climatic component is expected to represent meteorological phenomena beyond the monthly variations used in previous studies[28,29] and instead reflects responses to interannual variations (for example, climate extremes). In the case of Australia, positive trends in vegetation–rainfall sensitivity are likely to indicate a trend towards more-favourable and less-extreme climatic conditions (increased rainfall due to prevalent La Niña events)[34]. This is supporting a recovery from a series of consecutive dry years that led to the 'millennium drought' in large parts of Eastern Australia in the beginning of the twenty-first century[35].

In Southwest Africa, changing climatic conditions, especially a rise in temperature (Supplementary Fig. 9b), have been shown to impede the survival of larger woody plants and favour the spreading of smaller ones (woody encroachment) and more drought-tolerant but non-native species (alien species invasion)[10,36,37]. SeRGS captures such change in vegetation composition as it reveals higher average values for herbaceous vegetation (sparse vegetation, grasses and shrubs) as compared with woody vegetation (tree cover) (Supplementary Fig. 4). We show that a change in ecosystem composition, especially a replacement of large woody plants with shrubs, is expressed as a positive trend in vegetation–rainfall sensitivity. However, it remains an open question whether such a positive change would also be associated with sustainable environmental improvement, benefiting the ecosystem and people's livelihoods[4]. In fact, despite observed positive trends, certain aspects of ecosystem properties, for example, the loss of biodiversity or impact on groundwater[38], are not accounted for. Moreover, grasslands in dryland areas play an important role in carbon sequestration as they store high rates of carbon mainly below ground. Here, the carbon is able to persist through potential disturbances such as fire, whereas carbon stored in small trees and bushes (promoted by woody encroachment) is more vulnerable to external influences[39]. Similarly, positive trends in vegetation–rainfall sensitivity can also be seen in the eastern part of the North American tropical drylands that are associated with climatic drivers (for example, a rise in temperature (Supplementary Fig. 9b)).

The positive trends generally found in regions controlled by climatic drivers may again be related to an encroachment of smaller woody plants. These trends may also reflect more-productive systems in response to an increase in atmospheric CO_2 concentration[40]

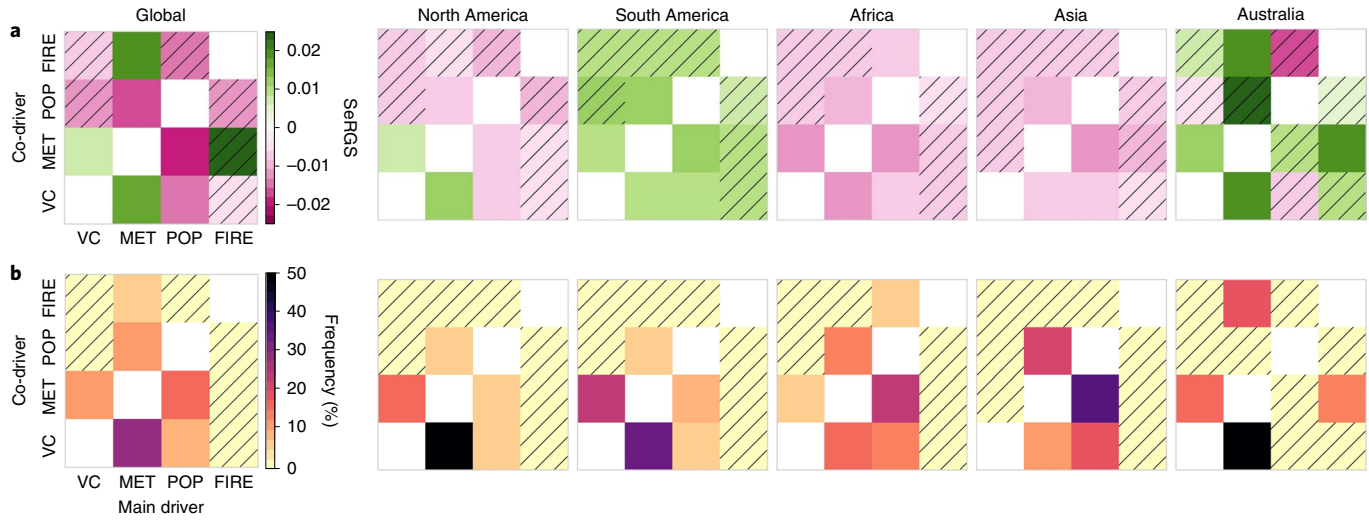

Fig. 3 | Driver combinations and contribution to changes in vegetation–rainfall sensitivity. a,**b**, The matrices show the median trend in vegetation–rainfall sensitivity (**a**) and associated frequency (**b**) for a given driver combination globally and for each continent. Main drivers are represented at the *x* axis and the second-most important (co-) drivers at the *y* axis. Hashed tiles show combinations that occur less than 5% (based on all pixels that show a significant trend (Mann–Kendall test, $P < 0.05$) in vegetation–rainfall sensitivity within the dryland mask at 0.05° spatial resolution).

as it has been suggested that the water use efficiency of vegetation increases as atmospheric CO_2 concentrations rise[41], especially in drylands and in tropical regions[42]. This CO_2 fertilization effect may, as well, have an impact on our estimated trends in the vegetation–rainfall sensitivity. However, the contribution of CO_2 fertilization is not expected to produce spatially varying patterns in vegetation–rainfall sensitivity for tropical dryland ecosystems. The role of CO_2 is also difficult to quantify, as no spatially explicit dataset covering the study period exists.

Population pressure reduces vegetation–rainfall sensitivity

In contrast to the overall positive trends for areas controlled mainly by climatic variables, we find a clear and strong negative influence from population on changes in vegetation sensitivity to rainfall (Fig. 3), indicating a change towards either less vegetation cover or vegetation being less responsive to rainfall. Overall, in areas where population is identified as the main (or co-) driver of change, the median trend in vegetation–rainfall sensitivity is negative, whereas other driver combinations relate mainly to positive trends (Fig. 3a). The most extensive areas where trends are population driven are located in large parts of sub-Saharan Africa and northern India (Fig. 2), largely overlapping with areas experiencing the highest increase in population and population density to the present date (Supplementary Fig. 7a), a development projected to continue in the future[43]. Population pressure on ecosystems can be both direct (for example, allocation of land for settlements or expansion of agricultural frontiers into natural ecosystems due to an increased demand for resources) and indirect (for example, loss of biological diversity)[44,45] and may be related to, for example, population growth, migration or armed conflicts[46]. In most of these population-driven areas, meteorological variables have been identified as dominant co-limiting factor (Figs. 2 and 3), and generally, climatic conditions have been reported to be more favourable in recent decades (that is, increased or stable water availability, Supplementary Fig. 9a), leading to an increase in vegetation productivity and large-scale greening trends (for example, 'greening Sahel')[47]. These greening trends, however, may also be related to structural changes in vegetation composition (Supplementary Fig. 4)[48] or increasing atmospheric CO_2[14,40]. Regardless of the causes, such continuous increase in vegetation productivity may create an offset in the vegetation–rainfall relationship, ultimately causing negative trends in SeRGS, despite a greening (Supplementary Fig. 3b). As such, changes in vegetation productivity are likely to further intensify or mitigate the negative trends in vegetation–rainfall sensitivity, depending on the nature of population-driven impacts on the ecosystem that may affect either herbaceous (for example, grazing) or woody (for example, deforestation) vegetation. A previous study found low sensitivity of vegetation to climatic variability and high ecological resilience (on the basis of time series analysis of monthly integrated vegetation and climatic data) in the regions identified here as population driven[29]. Our study demonstrates, however, that population pressure also plays a central role in the observed change in the sensitivity of vegetation to changes in rainfall in such regions and that human pressure is equally important for characterizing the vegetation response in addition to climate variability in many dryland areas. Thus, neglecting proxies of human impact as driving forces is likely to lead to biased conclusions.

Land-use/cover changes and vegetation–rainfall sensitivity

We find the largest contribution of vegetation cover change to changes in vegetation–rainfall sensitivity in large parts of South America (for example, Caatinga and Gran Chaco), sub-Saharan Africa (for example, Miombo woodlands) and parts of Western Australia (Figs. 2 and 3). Here, changes in vegetation cover are associated with a gain in short vegetation[33] and translate into positive trends in vegetation sensitivity to rainfall. These areas largely overlap with areas of agricultural intensification or conversion from woodland to agriculture[13,33]. Year-round farming practices lead to an increased but more rainfall-dependent vegetation productivity (rainfed crops) as compared with deciduous natural plants, which translates into a positive trend in SeRGS over time. Especially the South American dry Chaco has experienced a rapid intensification of agriculture since the 1970s (among others for global meat and soy production), going alongside heavy deforestation, causing increased carbon emissions and biodiversity loss[4,49,50]. Similarly, the Miombo woodlands, historically related to smallholder agriculture, have been increasingly converted into large-scale commodity crop cultivation[51,52]. Our analysis supports the human impact on these natural systems as population is often the associated co-driver in

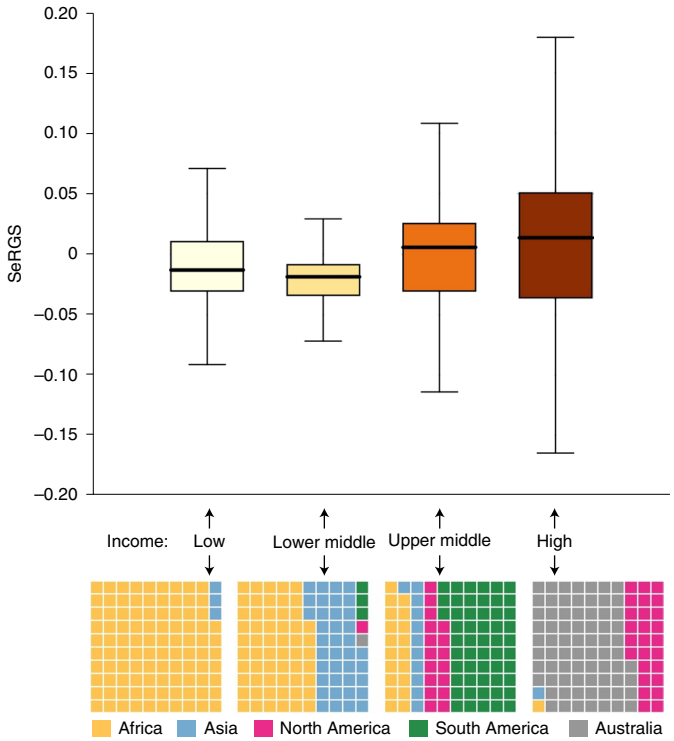

Fig. 4 | Changes in ecosystem functioning in relation to economic strength. Box plots are based on 5,000 randomly distributed pixels within each income group at 0.05° spatial resolution. Areas with a Human Footprint score <5 (indicating very low human pressure) have been excluded from the analysis (see Methods). Boxes represent the interquartile range (IQR) of the data with whiskers extending to 1.5 IQR to both sides, and median values are shown as a black line. The waffle plot shows the share of the continents within each income group where one tile represents 1%. A map showing median SeRGS trends per country superimposed on the per-pixel SeRGS trends and the value range of SeRGS trends per income group are shown in Supplementary Fig. 8c,d.

these regions (Fig. 3). Contrasting the overall negative impact of population on the land due to direct pressure from a high and growing population density as seen in other areas (for example, Sahel), the human imprint here rather reflects human land management. Intense land management (agriculture intensification and conversion) and an associated increase in vegetation (crop) productivity, which is fuelled by trends towards the use of mechanization, fertilizer, better-quality seeds or quick-growing hybrid cultivars, is often referred to as cropland greening[13]. However, whether such a development represents actual environmental improvement can be questioned and calls for a more nuanced assessment, including a broader range of both ecosystem property indicators including biodiversity and an assessment of sustainability of land transitions and practices.

Economic inequality and vegetation–rainfall sensitivity

Negative median trends in the vegetation–rainfall sensitivity are found in low- to lower-middle-income countries, and similarly, positive median trends are observed in upper-middle- and high-income countries (as classified by the World Bank, Supplementary Fig. 8a) (Fig. 4), particularly for areas of low to medium human footprint levels (Supplementary Fig. 8b). Previous research outlined that, in general, low-income countries are more vulnerable to climate change (for example, rising temperatures[53]) and may prioritize short-term effects of adaptation over more-sustainable mitigation processes due to an unfavourable economic situation and cost–benefit considerations. At the same time, high-income countries have a higher capability to counter possible adverse effects of climate change on agriculture, human health and ecosystems[54]. The observed differences might also reflect land-use practices and ecosystem management, where large-scale transformations from natural to arable land (as shown to be responsible for large parts of positive trends in vegetation–rainfall sensitivity) require economic resources (human and non-human) and certain infrastructure (for example, farm mechanization, the use of fertilizers and high-quality seeds[55]) more easily accessible in high-income countries. Similarly, increased pressure from population growth in low-income countries may further fuel overexploitation of resources (for example, shortening of the fallow period), ultimately leading to land degradation, reflected in negative trends in vegetation–rainfall sensitivity.

Concluding remarks

One-third of tropical dryland ecosystems have shown significant changes ($P < 0.05$) in vegetation sensitivity to rainfall, that is, changes in vegetation biophysical processes in relation to water availability over recent decades. We link observed changes to potential climatic and anthropogenic drivers and bring a new level of comprehensive assessment of their interplay at global scale, further highlighting the importance of integrated assessment of both human and climate-change impacts in environmental and sustainability studies. We find pronounced geographical and economic differences regarding both changes in vegetation–rainfall sensitivity and potential drivers/driver combinations. Large parts of the world's poorest countries experience negative changes in vegetation–rainfall sensitivity, linked mainly to growing population pressure, whereas the vegetation sensitivity to rainfall of richer countries tends to improve, notably as a result of favourable climatic conditions and/or an intensification and expansion of agricultural lands. In addition, it has been suggested that changes in vegetation water usage and vegetation functioning as depicted by SeRGS may be indicative of the changing sensitivity (that is, reduced or increased vegetation resistance) of vegetation to environmental stressors[56]. If (combined) human and climatic stress continues to increase, thereby decreasing vegetation resistance, ecosystem services may be jeopardized and the ecosystem has a higher chance to switch to an alternative state[28]. Thus, identifying such areas is pivotal to highlight highly vulnerable regions and to contribute to sustainable land management. As such, future research on ecosystem functioning should incorporate both metrics of vegetation–rainfall sensitivity and other aspects of vegetation functioning, such as biodiversity or vegetation composition.

Methods

All datasets were harmonized to match the period from 2000 to 2015, which is the minimum overlap of all datasets used in this study. We resampled all datasets to 0.05° spatial resolution from their original resolution using cubic convolution[57].

A tropical dryland mask was derived in the following steps. We consider only environments that are predominantly water limited. This is the case when the relative importance of the water constraint (compared with radiation and temperature) is greater than 55% (ref. [58]), thereby excluding temperate drylands. In addition, we exclude areas receiving more than 1,000 mm mean annual rainfall, as in these areas a strong vegetation–rainfall relationship is likely to be hampered by other climatic variables. Following this, all areas classified as bare soil (200–202) or irrigated cropland (20) in the European Space Agency (ESA) Climate Change Initiative (CCI) Land Cover map 2015[59] and areas with an aridity index below 0.05 (hyper-arid areas), as derived from ref. [60], were removed. The remaining areas are referred to as global drylands (Supplementary Fig. 1). All input datasets were harmonized, and all processing has been done within this global tropical dryland area.

MODIS reflectance data. We used MODIS (MOD09GQ, collection 6, available from ref. [61]) eight-day composite reflectance data[62] at 250 m original spatial resolution to calculate the NDVI as a proxy for vegetation productivity[63,64] for the period 2000–2015. The NDVI has been shown to be closely related to vegetation productivity or net primary production in drylands[65–67]. We resampled data from the original resolution to 0.05° using the median and calculated the annual sum. In addition, we used the VIP product, available from ref. [68]. At a spatial resolution of 0.05°, VIP provides consistent measurement of NDVI (and the enhanced

vegetation index) on the basis of data from MODIS and the Advanced Very High Resolution Radiometer that are used to derive phenological metrics such as the start and end of season or the cumulative NDVI over the growing season.

Rainfall data. There are many freely available precipitation datasets, of which comparative studies indicate MSWEP to be the most accurate as compared with station data[69–71]. MSWEP v.1[72] is a globally gridded, merged (from gauge, satellite and reanalysis data) precipitation dataset at 0.25° spatial resolution (available from http://www.gloh2o.org/), originally available at a temporal resolution of three hours from which we calculated annual sums. To account for spatial patterns in rainfall seasonality that may impact vegetation productivity (for example, rainfall in December may impact NDVI in March), we calculated the optimal rainfall sum on a per-pixel level. The optimal rainfall sum is calculated as rainfall totals accumulated over the growing season (GS, as defined by the VIP start and end of season) and over an additional period (months) before the GS. The number of additional months before GS was optimized per pixel and was set to attain the highest significant ($P < 0.01$) correlation between accumulated rainfall and vegetation productivity for the shortest accumulation period before GS.

Soil-water content and temperature data. We used data on soil-water content and two-metre air temperature from the fifth generation of European Centre for Medium-Range Weather Forecasts reanalysis climate data (ERA5) for this study[73] (available at https://cds.climate.copernicus.eu/cdsapp#!/dataset/reanalysis-era5-land?tab=overview). The original data are provided monthly on a regular grid at 0.1° spatial resolution from which we estimated averages over the growing season on the basis of the metrics from VIP. As these metrics indicate the day of the year of start and end of season, the whole month was included to the growing season.

MODIS burned-area product. At 500 m spatial resolution, the MODIS burned-area product (MOD64A1) provides estimates of daily changes in surface reflectance from fire activity[74]. We calculated the fire occurrence for each pixel for every year within the period 2000–2015.

Land-cover data. Vegetation continuous field data were used in this study to represent continuous land-surface cover. Data are distributed through Land Processes Distributed Active Archive Center (https://lpdaac.usgs.gov/dataset_discovery/measures/measures_products_table/vcf5kyr_v001). Song et al.[33] provide this data as a fractional combination of vegetation functional types, that is, tree cover (TC), short vegetation (SV) and bare ground (BG), on the basis of the Advanced Very High Resolution Radiometer at 0.05° spatial and yearly temporal resolution. The TC layer includes tall vegetation ≥5 m in height, and shorter vegetation such as small trees, shrubs and bushes are represented within the SV layer. However, within this categorization of land-surface cover, TC barely exists in arid savannah landscapes (for example, the Sahel, Southern Africa). As such, SV and BG are negatively related, and a change in BG over time is reflecting the same change in SV (inverted) (Supplementary Fig. 10b). In more-densely vegetated areas, however (for example, Gran Chaco), where the fraction of BG is small or non-existent, TC and SV are inversely related (Supplementary Fig. 10a). To avoid this duplicate land-cover information in the assessment of the relative importance of each driver, we included only two out of three classes in our analysis. As such, we are able to represent the vegetation cover of drylands (or trends herein) with the TC and BG layers. BG is selected over SV as (1) the SV layer is the one most frequently carrying redundant information in relation to the classes of either TC or BG, and (2) we want to retain information about the full continuum of vegetation cover from trees to bare ground.

Population data. The fourth version of the Gridded Population of the World (GPWv.4) represents modelled data on the distribution of human population (count and density) at various spatial scales (available at https://sedac.ciesin.columbia.edu/data/collection/gpw-v4). The dataset is based on census data collected around 2010 and has been extrapolated to population estimates for the years 2000, 2005, 2010, 2015 and 2020[75]. For this study, we use the available datasets 2000–2015 at ~1 km spatial resolution and linearly interpolate the missing years to create a continuous annual time series.

Global income data. Global income groups are based on gross domestic product in US$$_{2015}$ as provided by the World Bank[76].

Dryland vegetation functioning and water availability (SeRGS). In tropical drylands, where vegetation productivity is tightly linked to the availability of water (mainly through rainfall), alterations in the VRR over time may be used as an indicator for altered sensitivity of vegetation to rainfall, one major aspect of vegetation functioning. Analysing the sequential linear regression slopes (SeRGS) of the VRR over a time series of remote-sensing data has been introduced as an effective tool to do so[25] . The advantage of this method is that instead of using pure vegetation productivity-based indices, it incorporates rainfall as the driving force and already 'normalizes' for interannual variations in rainfall (under the assumption that more/less rainfall generates more/less vegetation), thereby better exposing the signal of the underlying causal processes. Such a normalization (or smoothing) effect was achieved by generating a spatially and temporally dynamic VRR through the application of a spatially and temporally moving window of 7 × 7 pixels and four years, respectively (see ref. [25] for details and parametrization). For all pixels within a given window, a linear regression between NDVI and rainfall was fitted, and the regression slope was assigned to the centre pixel of the spatially moving window and centre year of the temporal window, respectively. This results in a time series of slopes, hereafter called the SeRGS time series. When more than two-thirds of the pixels are of low quality, the regression is not fitted and no data are assigned to the centre pixel. Finally, a Theil-Sen estimator (indicating trend directions in vegetation–rainfall sensitivity) was calculated for the SeRGS time series for all pixels having more than two-thirds valid pixels and no more than three consecutive missing values. As the annual integration of NDVI and rainfall on the basis of the calendar year may be appropriate to represent
the VRR in some regions, it may not be suitable in other regions. To account for regional differences in the VRR, we calculated the correlation between annually summed NDVI and rainfall and compared it with the correlation between seasonally integrated NDVI and the rainfall optimal sum on a per-pixel level. For each pixel, we chose the dataset combination that revealed the highest correlation (Supplementary Fig. 2) as input data to calculate SeRGS. SeRGS was then applied on tropical drylands using the respective NDVI and rainfall dataset from 2000 to 2015 at a spatial resolution of 0.05°. Examples of how SeRGS relates to NDVI and rainfall temporal dynamics are generically shown in Supplementary Fig. 3.

Relative importance of potential driving variables. To estimate the relative importance of various climatic and anthropogenic variables potentially driving annual variations and long-term changes in SeRGS, we used a multiple regression approach[29,77] (Supplementary Fig. 5). While SeRGS in itself normalizes vegetation productivity for variations in annual rainfall, other meteorological variables, such as temperature and soil-water availability, may influence vegetation biophysical processes and thereby the vegetation–rainfall sensitivity. Moreover, fire occurrence, vegetation cover (TC and BG) and population density were chosen as potential driving factors. To reduce any impact of collinearity between the predictor variables, a PCA and PCR were used to ultimately identify the relative importance of each of the driver variables in each pixel. On a per-pixel level, through the PCA, we transform the input variables, which have been normalized by the standard deviation into a set of new variables, the principal components, which are now uncorrelated but still explain all the variation in the data. Each of the components has scores and loadings, with the latter indicating the correlation between principal component and the input variables. We then performed a multiple linear regression with SeRGS as the dependent variable and the principal components as independent variables, multiplied the regression slope from the PCR with the respective loadings from the PCA and summed the absolute values of these scores. Thus, we obtained a per-pixel estimate of the relative importance of each potentially driving variable on SeRGS. To reduce complexity and ensure readability of the maps and figures, we grouped soil-water content and temperature to represent meteorological drivers as well as TC and BG to represent changes in vegetation cover as a whole and downscaled (using the majority) the map to 0.25° spatial resolution.

Vegetation sensitivity to rainfall and economic strength. We estimated median trends in vegetation sensitivity to rainfall, as shown by SeRGS, per income group (provided by the World Bank) at the country level. As human accessibility varies substantially between different regions of tropical dryland areas, we restricted the analysis to areas that actually experience human pressure (excluding areas with a human footprint score <5, indicating very low/low human pressure), thereby excluding, for example, parts of the Australian drylands (Supplementary Fig. 7b). The global human footprint[78] was used as an indicator for cumulative human pressure. Median SeRGS values were calculated on the basis of a randomly chosen subsample of 5.000 pixels per income group.

Data availability

The datasets analysed in this study are publicly available as referenced within the article. The data that support the findings of this study are available from the corresponding author upon reasonable request. Source data are provided with this paper.

Code availability

The codes used in the data analysis to calculate SeRGS as well as potentially related drivers are available at https://github.com/Frangi10ne/SeRGS.

References

1. Environment Management Group *Global Drylands: A UN System-Wide Response* (UN Department of Environment Management, 2011).

2. Gudka, M. et al. Conserving dryland biodiversity: a future vision of sustainable dryland development. *Biodiversity* **15**, 143–147 (2014).
3. Millennium Ecosystem Assessment *Ecosystems and Human Well-Being: Desertification Synthesis* (World Resources Institute, 2005).
4. Cherlet, M. et al. *World Atlas of Desertification* (Publication Office of the European Union, 2018).
5. IPCC *Special Report on Climate Change and Land* (eds Shukla, P. R. et al.) (IPCC, 2019).
6. Ji, F., Wu, Z., Huang, J. & Chassignet, E. P. Evolution of land surface air temperature trend. *Nat. Clim. Change* **4**, 462–466 (2014).
7. Huang, J., Guan, X. & Ji, F. Enhanced cold-season warming in semi-arid regions. *Atmos. Chem. Phys.* **12**, 5391–5398 (2012).
8. Zhang, W., Brandt, M., Tong, X., Tian, Q. & Fensholt, R. Impacts of the seasonal distribution of rainfall on vegetation productivity across the Sahel. *Biogeosciences* **15**, 319–330 (2018).
9. Maestre, F. T. et al. Increasing aridity reduces soil microbial diversity and abundance in global drylands. *Proc. Natl Acad. Sci. USA* **112**, 15684–15689 (2015).
10. Zhang, W. et al. Ecosystem structural changes controlled by altered rainfall climatology in tropical savannas. *Nat. Commun.* **10**, 671 (2019).
11. Grimm, N. B. et al. The impacts of climate change on ecosystem structure and function. *Front. Ecol. Environ.* **11**, 474–482 (2013).
12. Huang, J. et al. Dryland climate change: recent progress and challenges. *Rev. Geophys.* **55**, 719–778 (2017).
13. Chen, C. et al. China and India lead in greening of the world through land-use management. *Nat. Sustain.* **2**, 122–129 (2019).
14. Zhu, Z. et al. Greening of the Earth and its drivers. *Nat. Clim. Change* **6**, 791–795 (2016).
15. Andela, N., Liu, Y. Y., van Dijk, A. I. J. M., de Jeu, R. A. M. & McVicar, T. R. Global changes in dryland vegetation dynamics (1988–2008) assessed by satellite remote sensing: comparing a new passive microwave vegetation density record with reflective greenness data. *Biogeosciences* **10**, 6657–6676 (2013).
16. Abdi, A. M., Seaquist, J., Tenenbaum, D. E., Eklundh, L. & Ardö, J. The supply and demand of net primary production in the Sahel. *Environ. Res. Lett.* **9**, 094003 (2014).
17. Darkoh, M. B. K. The nature, causes and consequences of desertification in the drylands of Africa. *Land Degrad. Dev.* **9**, 1–20 (1998).
18. Pricope, N. G., Husak, G., Lopez-Carr, D., Funk, C. & Michaelsen, J. The climate–population nexus in the East African Horn: Emerging degradation trends in rangeland and pastoral livelihood zones. *Glob. Environ. Change* **23**, 1525–1541 (2013).
19. Huang, J., Yu, H., Guan, X., Wang, G. & Guo, R. Accelerated dryland expansion under climate change. *Nat. Clim. Change* **6**, 166–171 (2016).
20. De Boeck, H. J. & Grünzweig, J. M. Drivers and mechanisms of dryland ecosystem functioning emerging in more humid biomes under climate change. *Present. 2018 American Geophysical Union Fall Meeting 2018* abstr. B12B-06 (2018).
21. Reiss, J., Bridle, J. R., Montoya, J. M. & Woodward, G. Emerging horizons in biodiversity and ecosystem functioning research. *Trends Ecol. Evol.* **24**, 505–514 (2009).
22. Jax, K. Function and "functioning" in ecology: what does it mean? *Oikos* **111**, 641–648 (2005).
23. Sprugel, D. G. Disturbance, equilibrium, and environmental variability: what is 'natural' vegetation in a changing environment? *Biol. Conserv.* **58**, 1–18 (1991).
24. Fischer, R. A. & Turner, N. C. Plant productivity in the arid and semiarid zones. *Annu. Rev. Plant Physiol.* **29**, 277–317 (1978).
25. Abel, C., Horion, S., Tagesson, T., Brandt, M. & Fensholt, R. Towards improved remote sensing based monitoring of dryland ecosystem functioning using sequential linear regression slopes (SeRGS). *Remote Sens. Environ.* **224**, 317–332 (2019).
26. Ratzmann, G., Gangkofner, U., Tietjen, B. & Fensholt, R. Dryland vegetation functional response to altered rainfall amounts and variability derived from satellite time series sata. *Remote Sens.* **8**, 1026 (2016).
27. De Keersmaecker, W. et al. Assessment of regional vegetation response to climate anomalies: a case study for Australia using GIMMS NDVI time series between 1982 and 2006. *Remote Sens.* **9**, 34 (2017).
28. De Keersmaecker, W. et al. A model quantifying global vegetation resistance and resilience to short-term climate anomalies and their relationship with vegetation cover. *Glob. Ecol. Biogeogr.* **24**, 539–548 (2015).
29. Seddon, A. W. R., Macias-Fauria, M., Long, P. R., Benz, D. & Willis, K. J. Sensitivity of global terrestrial ecosystems to climate variability. *Nature* **531**, 229–232 (2016).
30. Abreu, R. C. R. et al. The biodiversity cost of carbon sequestration in tropical savanna. *Sci. Adv.* **3**, e1701284 (2017).
31. Brandt, M. et al. Ground- and satellite-based evidence of the biophysical mechanisms behind the greening Sahel. *Glob. Change Biol.* **21**, 1610–1620 (2015).
32. Schlaepfer, D. R. et al. Climate change reduces extent of temperate drylands and intensifies drought in deep soils. *Nat. Commun.* **8**, 14196 (2017).
33. Song, X.-P. et al. Global land change from 1982 to 2016. *Nature* **560**, 639–643 (2018).
34. Poulter, B. et al. Contribution of semi-arid ecosystems to interannual variability of the global carbon cycle. *Nature* **509**, 600–603 (2014).
35. van Dijk, A. I. J. M. et al. The Millennium Drought in southeast Australia (2001–2009): natural and human causes and implications for water resources, ecosystems, economy, and society. *Water Resour. Res.* **49**, 1040–1057 (2013).
36. Venter, Z. S., Cramer, M. D. & Hawkins, H.-J. Drivers of woody plant encroachment over Africa. *Nat. Commun.* **9**, 2272 (2018).
37. Stafford, W. et al. The economics of landscape restoration: benefits of controlling bush encroachment and invasive plant species in South Africa and Namibia. *Ecosyst. Serv.* **27**, 193–202 (2017).
38. Acharya, B. S., Kharel, G., Zou, C. B., Wilcox, B. P. & Halihan, T. Woody plant encroachment impacts on groundwater recharge: a review. *Water* **10**, 1466 (2018).
39. Bond, W. J., Stevens, N., Midgley, G. F. & Lehmann, C. E. R. The trouble with trees: afforestation plans for Africa. *Trends Ecol. Evol.* **34**, 963–965 (2019).
40. Lu, X., Wang, L. & McCabe, M. F. Elevated CO_2 as a driver of global dryland greening. *Sci. Rep.* **6**, 20716 (2016).
41. Keenan, T. F. et al. Increase in forest water-use efficiency as atmospheric carbon dioxide concentrations rise. *Nature* **499**, 324–327 (2013).
42. Schimel, D., Stephens, B. B. & Fisher, J. B. Effect of increasing CO_2 on the terrestrial carbon cycle. *Proc. Natl Acad. Sci. USA* **112**, 436–441 (2015).
43. United Nations Department of Economic and Social Affairs *World Population Prospects 2019: Highlights* (UN, 2019).
44. Crist, E., Mora, C. & Engelman, R. The interaction of human population, food production, and biodiversity protection. *Science* **356**, 260–264 (2017).
45. Ohana-Levi, N. et al. Time series analysis of vegetation-cover response to environmental factors and residential development in a dryland region. *GISci. Remote Sens.* **56**, 362–387 (2019).
46. Baumann, M. & Kuemmerle, T. The impacts of warfare and armed conflict on land systems. *J. Land Use Sci.* **11**, 672–688 (2016).
47. Hickler, T. et al. Precipitation controls Sahel greening trend. *Geophys. Res. Lett.* **32**, L21415 (2005).
48. Brandt, M. et al. Changes in rainfall distribution promote woody foliage production in the Sahel. *Commun. Biol.* **2**, 133 (2019).
49. Marinaro, S., Grau, H. R., Ignacio Gasparri, N., Kuemmerle, T. & Baumann, M. Differences in production, carbon stocks and biodiversity outcomes of land tenure regimes in the Argentine Dry Chaco. *Environ. Res. Lett.* **12**, 045003 (2017).
50. Gasparri, N. I. & Grau, H. R. Deforestation and fragmentation of Chaco dry forest in NW Argentina (1972–2007). *For. Ecol. Manage.* **258**, 913–921 (2009).
51. Ordway, E. M., Asner, G. P. & Lambin, E. F. Deforestation risk due to commodity crop expansion in sub-Saharan Africa. *Environ. Res. Lett.* **12**, 44015 (2017).
52. Jew, E. K. K., Dougill, A. J. & Sallu, S. M. Tobacco cultivation as a driver of land use change and degradation in the Miombo woodlands of south-west Tanzania. *Land Degrad. Dev.* **28**, 2636–2645 (2017).
53. Diffenbaugh, N. S. & Burke, M. Global warming has increased global economic inequality. *Proc. Natl Acad. Sci. USA* **116**, 9808–9813 (2019).
54. IPCC *Climate Change 2014: Impacts, Adaptation and Vulnerability* (eds Field, C. B. et al.) (Cambridge Univ. Press, 2014).
55. Jain, H. K. *Green Revolution: History, Impact and Future* (Studium Press LLC, 2010).
56. Hodgson, D., McDonald, J. L. & Hosken, D. J. What do you mean, 'resilient'? *Trends Ecol. Evol.* **30**, 503–506 (2015).
57. Herrmann, S. M., Anyamba, A. & Tucker, C. J. Recent trends in vegetation dynamics in the African Sahel and their relationship to climate. *Glob. Environ. Change* **15**, 394–404 (2005).
58. Nemani, R. R. et al. Climate-driven increases in global terrestrial net orimary production from 1982 to 1999. *Science* **300**, 1560–1563 (2003).
59. *Land Cover CCI: Product User Guide: Version 2.0* (ESA, 2017).
60. Zomer, A. & Trabucco, R. Global aridity index and potential evapotranspiration (ET0) climate database v2. *Figshare* https://doi.org/10.6084/m9.figshare.7504448.v3 (2019).
61. Vermote, E., Wolfe, R., NASA GSFC and MODAPS SIPS-NASA *MOD09GQ MODIS and the Terra Surface Reflectance Daily L2G Global 250m SIN Grid V006* (NASA EOSDIS LP DAAC, accessed February 2020); http://doi.org/10.5067/MODIS/MOD09GQ.006
62. Vermote, E. *MOD09A1 MODIS Surface Reflectance 8-Day L3 Global 500m SIN Grid V006* (NASA EOSDIS Land Processes DAAC, 2015).
63. Fensholt, R. & Proud, S. R. Evaluation of Earth Observation based global long term vegetation trends—comparing GIMMS and MODIS global NDVI time series. *Remote Sens. Environ.* **119**, 131–147 (2012).

64. Tian, F. et al. Evaluating temporal consistency of long-term global NDVI datasets for trend analysis. *Remote Sens. Environ.* **163**, 326–340 (2015).
65. Anyamba, A. & Tucker, C. J. Analysis of Sahelian vegetation dynamics using NOAA-AVHRR NDVI data from 1981–2003. *J. Arid. Environ.* **63**, 596–614 (2005).
66. Olsen, J. L., Miehe, S., Ceccato, P. & Fensholt, R. Does EO NDVI seasonal metrics capture variations in species composition and biomass due to grazing in semi-arid grassland savannas? *Biogeosciences* **12**, 4407–4419 (2015).
67. Tagesson, T. et al. Spatiotemporal variability in carbon exchange fluxes across the Sahel. *Agric. For. Meteorol.* **226–227**, 108–118 (2016).
68. *Multi-Sensor Vegetation Index and Phenology Earth Science Data Records* Version 4.0 (Vegetation Index and Phenology Lab, The University of Arizona, accessed February 2020); https://lpdaac.usgs.gov/products/vipphen_ndviv004/
69. Zwart, S. J., Mishra, B. & Dembélé, M. Satellite rainfall for food security on the African continent: performance and accuracy of seven rainfall products between 2001 and 2016. In *Remote Sensing and Hydrology Symposium* (2018).
70. Beck, H. E. et al. Global-scale evaluation of 22 precipitation datasets using gauge observations and hydrological modeling. *Hydrol. Earth Syst. Sci.* **21**, 6201–6217 (2017).
71. Burrell, A. L., Evans, J. P. & Liu, Y. The impact of dataset selection on land degradation assessment. *ISPRS J. Photogramm. Remote Sens.* **146**, 22–37 (2018).
72. Beck, H. E. et al. MSWEP: 3-hourly 0.25° global gridded precipitation (1979–2015) by merging gauge, satellite, and reanalysis data. *Hydrol. Earth Syst. Sci.* **21**, 589–615 (2017).
73. *Copernicus Climate Change Service (C3S) (2019): C3S ERA5-Land reanalysis* (Copernicus Climate Change Service, accessed February 2020); https://cds.climate.copernicus.eu/cdsapp#!/home
74. Giglio, L., Boschetti, L., Roy, D. P., Humber, M. L. & Justice, C. O. The Collection 6 MODIS burned area mapping algorithm and product. *Remote Sens. Environ.* **217**, 72–85 (2018).
75. Center for International Earth Science Information Network - CIESIN - Columbia University *Gridded Population of the World, Version 4 (GPWv4): Population Density, Revision 11* (NASA Socioeconomic Data and Applications Center (SEDAC), accessed February 2020); https://doi.org/10.7927/H49C6VHW
76. *Gross Domestic Product (GDP) (current US$) as of 2015* (World Bank, accessed July 2020); https://data.worldbank.org/indicator/NY.GDP.MKTP.CD
77. Zuur, A., Ieno, E. N. & Smith, G. M. *Analyzing Ecological Data* (Springer-Verlag, 2007).
78. Venter, O. et al. *Last of the Wild Project, Version 3 (LWP-3): 2009 Human Footprint, 2018 Release* (NASA Socioeconomic Data and Applications Center (SEDAC), accessed February 2020); https://doi.org/10.7927/H46T0JQ4

Acknowledgements

This research is part of the project entitled title 'Greening of drylands: Towards understanding ecosystem functioning changes, drivers and impacts on livelihoods', which is financed by the Danish Council for Independent Research (DFF, Grant ID: DFF-6111-00258). S.H. acknowledges the funding from the Belgian Federal Science Policy Office (Grant SR/00/339) and T.T. from the Swedish national Space board (SNSB Dnr 95/16). A.W.R.S. is partly funded on the ERC-2016-ADG HOPE project, W.D.K. on the eScience RETURN project, and A.M.A. was supported by the Swedish Research Council (Grant# 2018-00430).

Author contributions

C.A., S.H., T.T. and R.F. designed the study. C.A. conducted the analyses with support from S.H., T.T., W.D.K., A.W.R.S. and A.M.A.; C.A. drafted the manuscript with contributions by all authors.